Radiation Physics and Chemistry 218 (2024) 111549

Contents lists available at ScienceDirect

Radiation Physics and Chemistry

journal homepage: www.elsevier.com/locate/radphyschem

Evaluation of low-kV energy X-ray radiation effect on breast cancer cells incubated with gold nanoparticles capped with aminolevulinic acid, methyl aminolevulinate, and gamma-aminobutyric acid

Isabela Santos Lopes [a], Noemy Rodrigues Santos [b], Giovana Dias da Silva [b], Leonardo Camargo dos Santos [c], Maria da Penha Albuquerque Potiens [c], Daniel Perez Vieira [b], Lilia Coronato Courrol [a,*]

[a] Instituto de Ciências Ambientais, Químicas e Farmacêuticas, Departamento de Física, Universidade Federal de São Paulo, Diadema, São Paulo, Brazil
[b] Centro de Biotecnologia, Instituto de Pesquisas Energéticas e Nucleares, São Paulo, São Paulo, Brazil
[c] Centro de Metrologia das Radiações, Instituto de Pesquisas Energéticas e Nucleares, São Paulo, São Paulo, Brazil

ARTICLE INFO

Handling editor: Chris Chantler

Keywords:
Breast cancer
Gold nanoparticles
Aminolevulinic acid
Methyl aminolevulinate
And gamma-aminobutyric acid

ABSTRACT

Gold nanoparticles (AuNPs) have unique properties, including size-dependent optical and electronic characteristics, biocompatibility, and ease of functionalization, making them attractive for various diagnostic and therapeutic applications. The goal of this work was to verify the potential application of gold nanoparticles capped with aminolevulinic acid (ALA), methyl aminolevulinate (MALA), and gamma-aminobutyric acid (GABA) in low-energy X-ray diagnostics and therapy of breast cancer. ALA and MALA induce the accumulation of protoporphyrin IX (PpIX) in cancer cells. PpIX, in turn, can be excited by Cherenkov radiation, producing reactive oxygen species after energy or electron transfer from the triplet excited state of PpIX to molecular oxygen, which induces cell death by apoptosis or necrosis. The results indicated that ALA and MALA nanoparticles promoted reduced cell viability by approximately 20 % with X-ray irradiation at an energy level of 35 kV for 5 min. Breast cancer cells possess GABA receptors, allowing for targeted effects by GABANPs, which can enhance contrast and improve diagnostic potential. GABAAuNPs also demonstrated decreased cell viability in ~10 % following X-ray irradiation, making them a promising material for breast cancer diagnosis and treatment.

1. Introduction

Breast cancer stands as the most prevalent form of cancer affecting women on a global scale. According to data from the World Health Organization (WHO), in 2020, approximately 2.3 million women received diagnoses of breast cancer, resulting in 685,000 deaths globally (Arnold et al., 2022). The main known subtypes are grouped into four categories: Luminal A, Luminal B, human epidermal growth factor receptor positive (HER2+), and triple-negative (TNBC), dependent on expression of hormone receptors: estrogen receptor-positive (ER+), progesterone receptor positive (PR+), human epidermal growth factor receptor positive (HER2+). The Luminal A (ER+, PgR−/+, HER2-) subtype expresses hormonal receptors with low proliferative activity, while the Luminal B (ER+, PgR−/+, HER2+/−) subtype has higher proliferative activity and a challenging prognosis. HER2+ (ER+, PgR−/+, HER2+) tumors are aggressive and require targeted therapies, whereas TNBC (ER-, PgR-, HER2-) is heterogeneous and aggressive, demanding diverse therapeutic approaches(Hon et al., 2016).

Early identification plays a vital role in enhancing treatment results in the initial phases of breast cancer. Mammography is the most commonly employed imaging method for breast cancer screening and diagnosis, reducing mortality rates (Swaminathan et al., 2023). The American Cancer Society advises women to begin annual mammograms at 40 years old. Mammography machines typically operate from 25 kV to 35 kV, and 35 kV is a commonly used energy setting for breast imaging. At the low energies typically used for mammographic X-ray images, gold nanoparticles (AuNPs) exhibit remarkable attenuation, even at very low concentrations. AuNPs have been exploited as contrast agents, which enables high resolution (Torrisi et al., 2019).

Breast cancer treatment can be categorized into local treatment through surgery, radiotherapy, and systemic treatment via chemotherapy, hormone therapy, and biological therapy(Noor et al., 2021).

* Corresponding author.
E-mail address: lcourrol@unifesp.br (L.C. Courrol).

https://doi.org/10.1016/j.radphyschem.2024.111549
Received 18 September 2023; Received in revised form 20 December 2023; Accepted 22 January 2024
Available online 1 February 2024

The selection of treatment options depends on the disease's stage and the tumor's characteristics (Akram et al., 2017).

X-ray radiotherapy is a standard and effective treatment for various cancers, but it affects both tumors and healthy tissues, resulting in potential damage and side effects(Janssen et al., 2018). Efforts are being made to optimize radiotherapy to minimize these adverse effects and enhance cell survival in healthy tissue. The importance of optimizing radiation dose delivery processes to increase the efficacy of radiotherapy and minimize the dose required for tumor death is evident. One promising avenue is using AuNPs, which come in different shapes and sizes and have shown promise in drug delivery, imaging applications, and photothermal therapy(Allen et al., 2022; Amina and Guo, 2020). In breast cancer management, gold nanoparticles have been investigated for their potential to enhance radiotherapy dose (Fathy et al., 2018; Akter et al., 2023). The surface of these nanoparticles can be functionalized with various biomolecules, enabling target selectivity. Nanoparticles designed for radio enhancement can heighten the susceptibility of cancer cells to radiation(Bilynsky et al., 2022). When subjected to ionizing radiation, such as X-rays, gold nanoparticles have the potential to amplify the radiation dosage targeted at cancer cells, thus reducing harm to adjacent healthy tissue and augmenting the overall efficacy of therapy (Chen et al., 2020).

Aminolevulinic acid (ALA) gold nanoparticles have been studied, proving their theranostic applications(Goncalves et al., 2015, 2020). Combined with ALA, these nanoparticles cause a preferential accumulation of protoporphyrin IX (PpIX) in cancerous cells compared to normal cells. This difference in metabolism between normal and tumor cells allows for ALAAu-based photodynamic diagnosis and therapy. By transporting ALAAuNPs to specific cells, the diagnostic and radiotherapy dose can be significantly enhanced.

Methyl-5-aminolevulinate (MALA) is another compound like ALA used in clinical settings(Blanco et al., 2015; Mateus et al., 2014). Due to its methyl group, MALA is more selective for tissues and offers better results in photodynamic therapy (PDT) since it increases PpIX content in cells and improves cell uptake compared with ALA (Goncalvez et al., 2018).

The neurotransmitter gamma-aminobutyric acid (GABA), well-known for its role in the central nervous system, has also been found to be altered in cancer cells, particularly in breast cancer(Brzozowska et al., 2017). Research has indicated that stimulating GABA receptors can potentially suppress both the growth and spread of tumor cells (Yang et al., 2023). Numerous studies have indicated that individuals who exhibit higher GABA levels tend to experience more positive outcomes in terms of disease-free survival and overall survival when compared to those with lower GABA levels (Wu et al., 2023; Yang et al., 2023).

This study describes the GABAAuNPs synthesis for the first time, employing the photoreduction process. ALA, MALA, and GABA gold nanoparticles were employed in an *in-vitro* low-energy X-ray therapy.

2. Experimental

2.1. AuNPs synthesis

Tetrachloroauric acid ($HAuCl_4$), 5-aminolevulinic acid, Methyl δ-aminolevulinate, and gamma-aminobutyric acid were purchased from Sigma-Aldrich.

To prepare the ALAAuNPs, MALAAuNPs, GABAAuNPs, 45 mg of ALA/MALA/GABA, 15 mg of $HAuCl_4$ and 100 mg of Polyethylene glycol 10000 (PEG) were diluted in 100 mL of distilled water and followed by vigorous stirring for 5 min. ALA, MALA, and GABA solutions (10 mL) were illuminated for 2, 5, and 3 min, respectively, with a 300 Watts Xenon lamp from Cermax, with an intensity estimated to be 3.6 W/cm ^{2}.

All solutions have the pH adjusted to ~7.0 after NaOH solution irradiation.

2.2. Nanoparticle characterization

The UV–Vis absorption spectra were measured using a Shimatzu spectrophotometer with 1 cm quartz cells.

The shape and sizes of the AuNPs were determined using transmission electron microscopy (TEM) with a JEM-2100 Jeol instrument (Zeiss, Germany) at Laboratory of Microscopy and Microanalysis (LMM) is a multi-user laboratory located at the Center for Science and Technology of Materials (CCTM) of the Institute of Energy and Nuclear Research (IPEN).

The surface charges on the nanoparticles were measured using Zeta potential analysis, conducted with the Malvern Instruments Zetasizer (Worcestershire, UK) and the DKSH ZetaView at the multi-user laboratory from the Federal University of ABC.

FTIR spectra were recorded using a Shimadzu Prestige-21 spectrometer (Shimadzu Corp., Kyoto, JP) with a resolution of 2 cm^{-1} within the range of 4000 cm^{-1} to 400 cm^{-1}.

2.3. Cytotoxicity test

The MCF-7 breast tumor cells were cultured in RPMI 1640 medium supplemented with 10 % fetal bovine serum (FBS) and 1 % penicillin/streptomycin at 37 °C with 5 % CO_2. Cells were sub-cultured every 3 days at 70–80 % confluency and harvested using 0.25 % trypsin.

For the cytotoxicity analysis, 8×10^3 cells/wells were plated in 96-well flat-bottom plates and incubated for 24 h for adhesion and growth. Afterward, the cells were divided into different groups and incubated with ALAAu, MALAAu, and GABAAu at concentrations of 5 % (475 μL culture medium + 25 μL of NPs), 4 % (480 μL culture medium + 20 μL of NPs), 3 % (485 μL culture medium + 15 μL of NPs), and 2 % (490 μL culture medium + 10 μL of NPs).

The plates were then incubated for 48 h at 37 °C with 5 % CO_2. After incubation, the supernatant was removed, and the cells were washed with PBS before being incubated for another 24 h in RPMI medium.

Cell viability was assessed using the 3-(4,5-dimethylthiazol-2-yl)-5-(3-carboxymethoxyphenyl)-2-(4-sulfophenyl)-2H-tetrazolium, MTS (CellTiter 96® AQueous MTS Reagent). The absorbance at 490 nm was measured and is directly proportional to the number of live cells in the culture. The results were statistically compared using ANOVA and the Dunnett test against negative controls (NaCl 5 %) or positive controls (DMSO 10 %). The percentage of cell viability was calculated after background absorbance correction and blank absorbance subtraction as follows:

% Cell viability = 100 x (Experimental well absorbance/untreated control well absorbance).

2.4. Quantification of PpIX fluorescence by Hight content screening (HCS)

The High Content Screening (HCS) quantification assay was carried out in collaboration with the Genetics and Molecular Hematology Laboratory, Hospital das Clínicas, Faculty of Medicine, University of São Paulo, USP.

The assay was performed in 96-well plates (Cornig) with 2×10^4 cells/well. The cells were maintained for 24 h in an oven (37 °C and 5 % CO_2) for adhesion. Subsequently, the culture medium was replaced with a nanoparticle solution (10 μL of ALAAu and MALAAu in 40 μL of culture medium), which was then subjected to a 24 h incubation in an oven. Following this exposure period, the cells underwent a PBS wash and a 1 μL/well application of Hoechst 3342 fluorescence dye (at a 1/100 dilution). For each well, nine sites were imaged, and this process was repeated in three separate wells for each treatment. Cells displaying PpIX fluorescence were identified using the cell scoring functionality

within the MetaXpress software.

2.5. Radiotherapy procedure

After analyzing the results obtained from the serial dilution, the concentrations for the treatment were selected. The experiment was conducted using two plates - one for irradiated samples and the other as a control plate.

Studied groups.

A. Cell control (CC) - n = 32
B. Negative control: 5 % NaCl solution - n = 8 (Total volume = 1000 μL, comprising 950 μL of culture medium + 50 μL of NaCl)
C. Positive control: 10 % DMSO solution - n = 8 (Total volume = 1000 μL, comprising 900 μL of culture medium + 100 μL of DMSO)
D. ALAAuNPs, MALAAuNPs, GABAAuNPs (n = 8 for each group). The concentration of NPs used in this experiment did not induce cytotoxicity.

2.5.1. Experimental Timeline

Day 1: Cells were plated in a 96-well plate at a density of 5000 cells per well. The plate was then incubated at 37 °C in a 5 % CO_2 atmosphere for 48 h to allow for adhesion and growth.

Day 2: After 48 h, the culture medium in the wells was replaced with 100 μL of the respective nanoparticles solutions at their proper concentrations. The plate was again incubated at 37 °C with 5 % CO_2 for 24 h.

Day 3: After the 24 h incubation, the wells were washed with 100 μL of PBS. Then, 20 μL of PBS per well was added to prepare the samples for irradiation. The plates were positioned vertically 1 m away from the beam exit, as per the specified norms, within the radiation field of 12 cm diameter, aided by calibrated lasers. The X-ray beam quality simulating the energy range of a mammography device was used. The radiation reference for mammography was implemented in the Pantak/Seifert system, traceable to the German primary laboratory, Physikalisch-Technische Bundesanstalt (PTB). The parameters for the quality RQR - 4M are listed in Table 1.

An X-ray camera using the Radcal RC6M Series ionization chamber was employed to determine the X-ray beam characteristics. The camera was calibrated in the PTB with a measurement uncertainty of ±0.96 %, and the Keithley 6517A Electrometer was used with an uncertainty of ±2.0 % (Standard IEC61267). The camera was positioned at 1m from the source, with collimators measuring 34 mm and 50.8 mm and a field diameter of 12 cm.

The plate was irradiated for 5 min, resulting in an entry dose of approximately 96 mGy. The control plate underwent the same conditions as the irradiated plate for comparison purposes.

After irradiation, the wells were washed, and 100 μL of culture medium per well was added. The plate was incubated at 37 °C within an atmosphere containing 5 % CO_2 for a duration of 24 h.

4th day: After 24 h of incubation, the wells were washed with PBS. A solution consisting of 2 mL of MTS, 100 μL of phenazine methosulfate (PMS), and 9.9 mL of culture medium was prepared. Then, 100 μL of the prepared solution was added per well.

After a 2 h incubation period, the spectrophotometer was used to measure the readings.

Table 1
Parameters and quality implemented in the Pantak/Seifert system.

Quality	kV	mA	CSR (mmAl)	Filtration (mm)	kerma rate (mGy/min)
RQR - 4M	35	10	0.41	0.07 Mo	19.2

2.5.2. Statistical analysis

All studies were performed in triplicate. The results were statistically compared (ANOVA and Dunnett test) with controls.

3. Results

3.1. Nanoparticles characterization

The absorbance spectra of the ALAAu, MALAAu, and GABAAu nanoparticles are shown in Fig. 1a. The ALAAuNPs and MALAAuNPs presented the SPR (surface plasmon resonance) peak around 544 nm. In contrast, GABAAuNPs presented the SPR band at ~521 nm.

Fig. 1b shows the TEM images of gold nanoparticles. ALAAu e MALAAu are spherical, but GABAAuNPs present a worm-like shape.

Fig. 1c shows the FTIR of the study nanoparticles, demonstrating some similarities in the spectra and presence of amino acids on the surfaces of the nanoparticles. The data indicate that the synthesis mechanism of gold nanoparticles with the three different ligands occurred similarly.

Table 2 compares the Zeta potential and polydispersity index of the ALAAu, MALAAu, and GABAAu nanoparticles. Similar values were found. The nanoparticles have negative surface charges and similar stabilities.

3.2. Cytotoxicity study

The cytotoxicity effects of ALAAu, MALAAu, and GABAAu nanoparticles in MCF-7 cells can be observed in Fig. 2, where the percentage of cell viability is plotted in function of the percentage of nanoparticles present in the culture medium added in each well. The results showed that ALAAuNPs and MALAAuNPs presented toxicity at 4 and 5 % concentrations, but GABAAuNPs did not present toxicity in the studied concentrations.

3.3. PpIX fluorescence

ALAAu/MALAAu uptake and its subsequent transformation into PpIX within the cellular environment was monitored by PpIX fluorescence analysis performed by High Content Screening in breast tumor cells. In the obtained images, shown in Fig. 3a, it is possible to see the PpIX fluorescence in red inside the cells incubated with ALA, MALA, ALAAu and MALAAuNPs for 4 and 24 h. The cells were also stained with the fluorescent dye Hoechst 3342, which marks all viable cells in blue. In the control group, the cell nuclei exhibited distinct blue staining with no detectable red emission visible in the imagery. However, in the presence of nanoparticles, a decrease in the cell count was noted, and some cells displayed a noticeable red emission, indicative of the conversion to PpIX. It was observed that cells treated with ALAAu or MALAAu, presented an increased concentration of PpIX compared to control cells. Fig. 3b reveals differences in PpIX fluorescence percentage after 4h and 24h for ALAAu and MALAAuNPs, suggesting altered ALA uptake or processing. Further, Fig. 3c shows no significant difference in fluorescence content between cells incubated with ALA and ALAAuNPs for 24h.

3.4. X-ray irradiation

The results obtained from irradiating MCF-7 for 5 min with 35 KV X-rays are shown in Fig. 4. The results demonstrated that the irradiation of cells incubated with ALAAuNPs and MALAAuNPs reduced cell viability by approximately 22.9 % and 18.7 %, respectively, when compared to non-irradiated cell groups (p-values$<$0.0001). The combination of GABAAuNPs and X-ray irradiation decreased cell viability by about 9.7 %, which was statistically significant (p-value $<$0.01) when compared to non-irradiated cells. The control group and positive and negative controls exhibited no changes during the 5-min irradiation period.

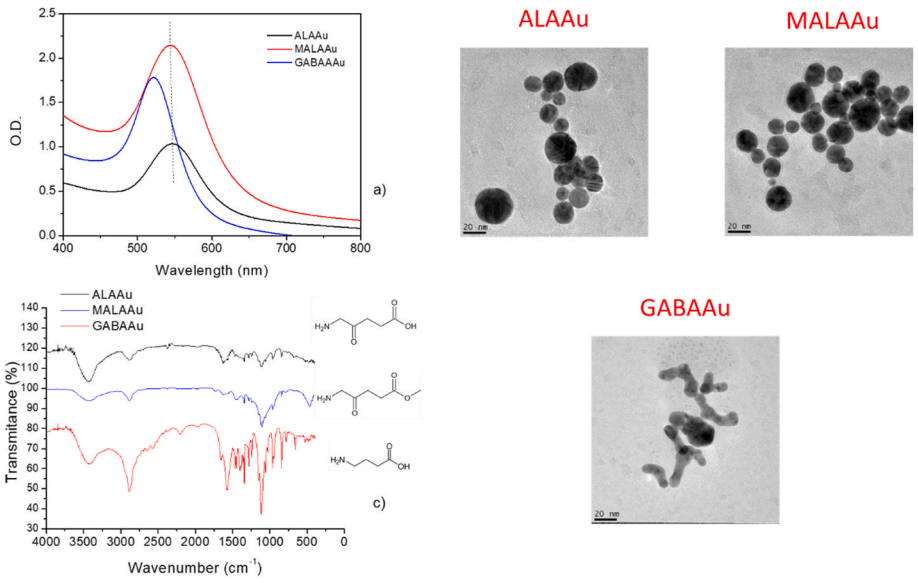

Fig. 1. a) UV–Vis spectra; b) TEM images and c) FTIR of ALAAu, MALAAu and GABAAuNPs.

Table 2
Zeta potential and polydispersity parameters of ALAAu, MALAAu, and GABAAu nanoparticles.

Parameter	ALAAu	MALAAu	GABAAu
Zeta potential (mV)	−23.1 ± 1.0	−21,9 ± 0,98	−25.1 ± 2.0
PDI	0.483	0.437	0.333

4. Discussion

Mammograms are generally considered safe; however, like all medical procedures involving radiation, they expose the breast to low X-rays (Diffey, 2017). Nonetheless, the benefits of early breast cancer detection through mammography far outweigh the potential risks for most women.

Utilizing low-dose X-rays generates detailed images of breast tissues, enabling early detection and prevention of breast cancer even before physical symptoms arise (Lebron-Zapata and Jochelson, 2018). In contrast to screening mammography, diagnostic mammograms provide more in-depth and targeted assessments. They are carried out when a woman experiences a mass, breast discomfort, discharge from the nipple, or abnormalities found during screening mammography (Schulz-Wendtland et al., 2009). Diagnostic mammography allows for a closer examination of breast tissues to determine the nature of any detected abnormality (Perry et al., 2019).

Several contrasts are involved in mammography, which is crucial in interpreting the images and detecting abnormalities (Perry et al., 2019). These contrasts refer to the differences in appearance between various types of tissues within the breast, and they are essential for distinguishing normal breast structures from potentially suspicious or cancerous lesions (Lorente-Ramos and Arman, 2022).

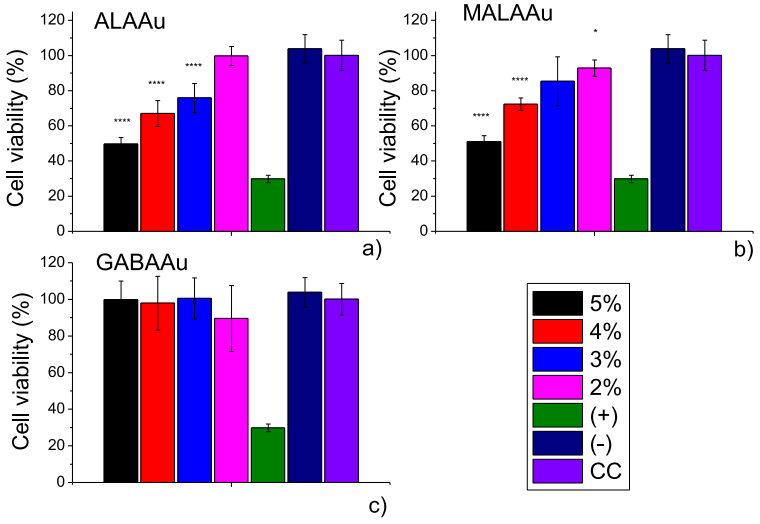

Fig. 2. Cell viability test in MCF-7 lineage, incubated for 24 h with a) ALAAu, b) MALAAu and c) GABAAuNPs. Data were compared using the ANOVA test followed by the Dunnett test, with p (****): p-value <0.0001, (*):p-value<0.01.

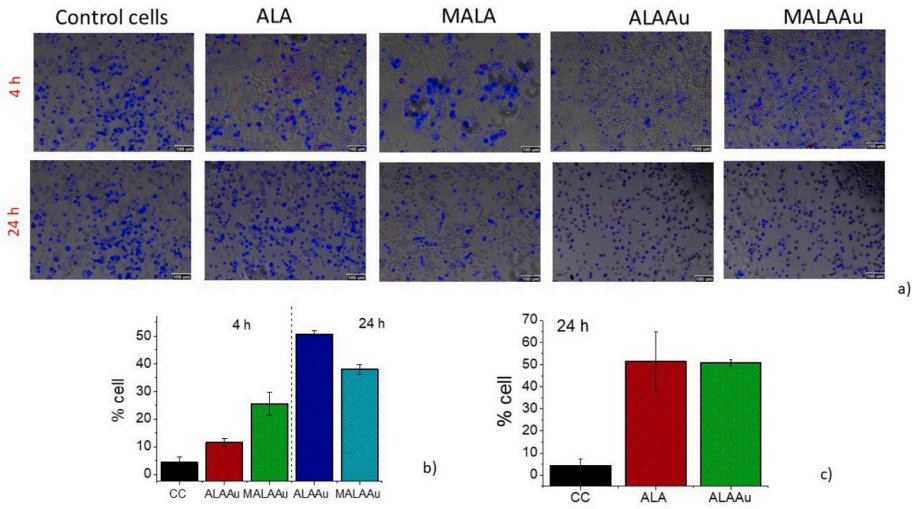

Fig. 3. a) HCS images obtained of MCF-7 cells and cells incubated for 4 h and 24 h with ALA. MALA, ALAAuNPs and MALAAuNPs. The cells were stained with Hoechst 3342, 2 h before imaging. b) The percentage of PpIX fluorescence in the red region around 675 nm, in cells marked. c) comparison between ALA and ALAAuNPs incubation.

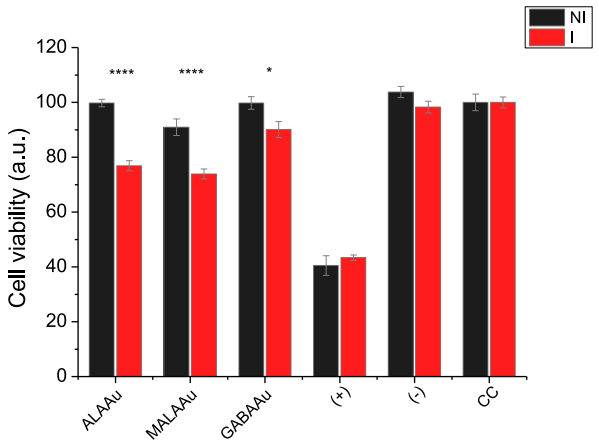

Fig. 4. MCF-7 viability after incubation with ALAAu, MALAAu, and GABAAu for 24 h not irradiated and irradiated with low-energy X-rays. Data were compared using the ANOVA test followed by the Dunnett test. (****): p-value <0.0001, (*):p-value<0.01.

Gold nanoparticles have gained interest in breast mammography due to their unique properties and potential applications (Chen et al., 2022). They can interact with X-rays, making them promising contrast agents for enhancing the detection and diagnosis of breast cancer in mammography(Hsu et al., 2020).

Regarding diagnosis, AuNPs can enhance the contrast between malignant and adjacent healthy tissue on mammography. This effect is primarily attributed to the high atomic number of gold (Au) and its ability to absorb X-rays more effectively than surrounding tissues (Piccolo et al., 2022). AuNPs enter cancer locations through the enhanced permeation and retention (EPR) effect, which takes advantage of the leaky vasculature and poor lymphatic drainage of tumor tissues (Xu et al., 2023). Engineered AuNPs are administered to a patient and accumulate in the tumor tissue. When an X-ray beam passes through the breast during mammography, the gold nanoparticles preferentially absorb more X-rays than the surrounding tissue. This differential absorption contrasts the tumor (where gold nanoparticles accumulate) and the healthy tissue (which absorbs fewer X-rays), making it easier to locate the tumor. The enhanced contrast provided by the gold nanoparticles can help to detect smaller tumors or lesions that might be challenging to see on a standard mammography, leading to a more accurate breast cancer diagnosis (Chen et al., 2020). AuNPs are nontoxic based on various *in vitro* and *in vivo* studies(Fratoddi et al., 2015; Kurapov and Bakhtenko, 2018). In particular, studies investigating AuNPs as an X-ray contrast agent have shown that AuNPs larger than 1.9 nm were nontoxic *in vivo* at doses ranging from 79 to 500 mg/kg while enabling successful contrast-enhanced imaging(Hsu et al., 2020).

Conjugating ALA or MALA with AuNPs enables a selective uptake by cancer cells. These cells have increased expression of ALA transporters (PEPT2, PEPT1, PAT1, TauT, and GAT2), which are involved in ALA uptake, facilitating the uptake of ALA/MALAAuNPs (Yang et al., 2015). In cells incubated with ALAAu or MALAAu, the abundant PpIX production cannot be quickly converted to its final product, heme, and therefore accumulates within cells(Blanco et al., 2015; Sachar et al., 2016; Zhang et al., 2015; Goncalves et al., 2020). The results shown in Fig. 3 confirm that ALA and MALA on the surface of NPs were metabolized to PpIX Fig. 3b demonstrates that cells incubated with MALAAuNPs have a higher PpIX fluorescence intensity than ALAAuNPs, suggesting more efficient uptake or conversion of ALA to PpIX. Interestingly, Fig. 3c shows that despite the decrease in viable cells observed previously, the overall PpIX content in cells treated with ALA and ALAAuNPs is similar. This suggests that ALAAuNPs may deliver ALA more effectively within cells, leading to increased cytotoxicity and decreased viability, even though total PpIX levels remain comparable. In the case of GABA-functionalized gold nanoparticles, since breast cancer cells have GABA receptors, GABA attached to the surface of the nanoparticles will be guided to bind specifically to receptors overexpressed in breast cancer cells. This targeted approach aims to increase the specificity and accuracy of mammography imaging for breast cancer. This is the first time GABAAuNPs were synthesized and studied in cancer cells. The particles are stable and have good stability.

Regarding therapy, X-ray therapy, or radiotherapy, is a standard treatment modality for breast cancer. The presence of AuNPs can potentially decrease the overall radiation dose required for breast cancer treatment, as demonstrated in studies by Nagi et al. (2017) and Torrisi et al. (2019) (Nagi et al., 2017; Torrisi et al., 2019). High-energy radiation interacting with AuNPs can trigger the emission of secondary electrons or Auger electrons (predominant for inner shells other than the K orbital) and photons (predominantly K-shell transitions)(Casta et al., 2015). Auger electrons or fluorescent X-rays arise from the relaxation of atoms following the ejection of electrons, as electrons from higher energy levels move to lower energy states, releasing energy. Auger electrons generate significantly increased ionization density within a

confined region. This is advantageous because it minimizes the risk of damage to healthy tissues. While the total radiation dose is lowered, using AuNPs results in an increased radiation dose specifically targeted to the tumor site. The AuNPs serve as enhancers or amplifiers of the effect of the radiation at the tumor site, rendering it more lethal to cancer cells while preserving the integrity of surrounding healthy tissues (Kuncic and Lacombe, 2018). In recent years, several research groups have explored the potential of photodynamic therapy (PDT) as an alternative to conventional surgical methods, such as breast-conserving surgery and complete mastectomy, for the treatment of breast cancer (Ismael et al., 2020). PDT uses a photosensitizing agent and light to generate cytotoxic reactive oxygen species (ROS) in target tissue. The penetration depth of light is limited, which restricts the use of PDT to superficial lesions or lesions accessible through endoscopic techniques.

Cherenkov radiation-induced photodynamic therapy (CR-PDT) is a promising alternative to traditional PDT due to its ability to generate reactive oxygen species (ROS) deep within tissues and has been described in the literature (Cline et al., 2019; Blum et al., 2020; Yang et al., 2022). Cherenkov radiation (CR) is a luminescence produced when a charged particle, such as an electron, travels through a medium at a speed greater than the phase velocity of light in that medium (Shaffer et al., 2017). Monte Carlo simulations suggest a Cherenkov fluence rate in the range of 1–100 μW cm^{-2} per Gy s^{-1}(Glaser et al., 2015). This range partially overlaps with the effective fluence range for low-dose-rate PDT, as demonstrated by Gonzales et al., who showed PDT efficacy with 15 μW/cm^2 at specific wavelengths using ALA as a photosensitizer(Gonzales et al., 2014). While further investigation is needed, these findings suggest that X-ray-driven Cherenkov radiation has the potential for PDT activation, warranting further research and optimization.

Bright spots were observed from ALAAuNPs diluted 50 % with culture medium irradiated with X-ray in the conditions described in Table 1, indicating radiation production (upper portion of Fig. 5). However, Cherenkov light is not emitted by the secondary electrons generated by X-ray photons <200 KeV(Yamamoto, 2021; Yamamoto et al., 2016). According to Yamamoto, the luminescence of water is a stable and reproducible luminescence similar to that of Cherenkov radiation, involving the dipole interaction between moving radiation (electrons) and electrons within molecules(Yamamoto et al., 2018). The light spectrum of the luminescence of water is $\sim 1/\lambda^2$, where λ is the wavelength of light(Yamamoto, 2021). Fig. 5 (bottom of the Figure) shows the luminescence of water spectrum compared with the normalized absorption spectrum of a PpIX solution prepared in acetone. So, the optical photon emission from the radicals produced in water is probably the source of radiodynamic therapy (RDT). This luminescence can excite PpIX from the singlet ground state to an excited singlet state, followed by intersystem crossing to an excited triplet state(Takahashi et al., 2013). The energy or electrons are transferred to oxygen molecules via type I and II reactions, generating reactive oxygen species (ROS), which causes cellular damage that leads to tumor cell death (Gutowski and Kowalczyk, 2013).

We demonstrated that ALA/MALAAuNPs reduced cell viability by around 20 % after 5 min of low-energy X-ray irradiation. In this case, the ROS triggered by Auger electrons emitted from the gold nanoparticles was enhanced by ROS produced from PpIX excitation. For GABAAuNPs, only ROS triggered by Auger electrons emitted was achieved, and a decrease in cell viability was ~10 %. Even a small amount of cell death can significantly impact tumor growth and can be achieved in a simple mammography procedure.

Fig. 5 illustrates the procedures and potential uses of ALAAu, MALAAu, and GABAAuNPs, as theranostic material enhancing diagnosis and RDT (ALA/MALAAu) or radiotherapy (GABAAu) for breast cancer.

The synthetic production of ALA/MALAAu, and GABAAuNPs present several potential economic, medical, and technological advantages.

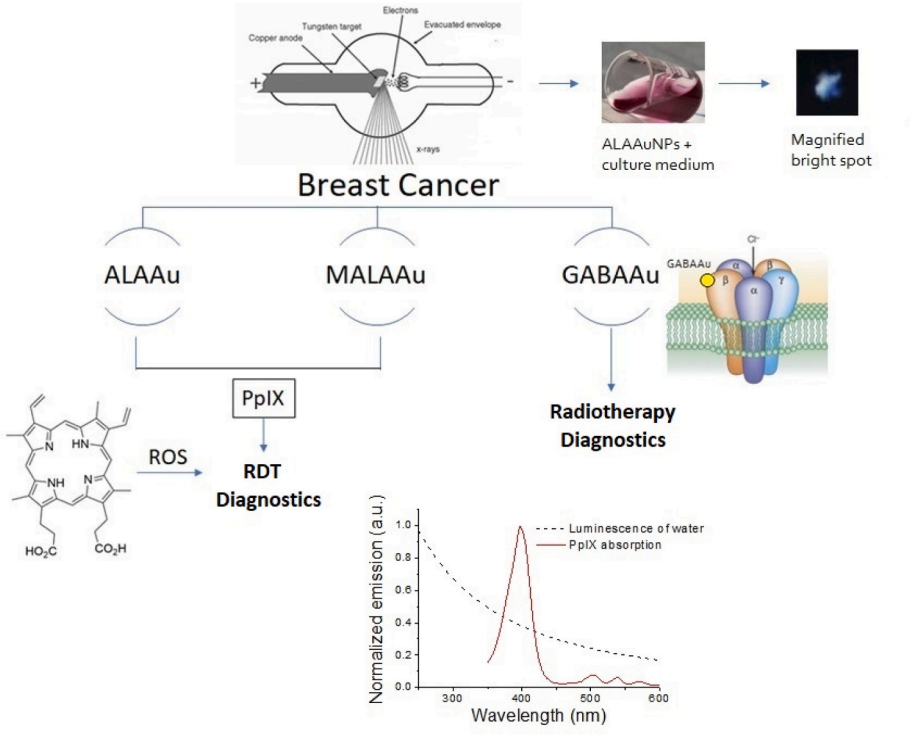

Fig. 5. Illustration depicting the diverse processes and potential applications of ALAAu, MALAAu, and GABAAuNPs. ALA/MALAAuNPs showcase versatility for diagnostics and Radiodynamic Therapy (RDT), where Protoporphyrin IX (PpIX) is stimulated by the luminescence of water during RDT. Meanwhile, GABAAuNPs find applications in both radiotherapy and diagnostics. The upper portion of the Figure captures the striking emergence of bright spots from ALAAu nanoparticles dispersed in a culture medium under X-ray irradiation. In contrast, the lower section juxtaposes the luminescence spectrum of water ($1/\lambda^2$) with the normalized absorption spectrum of a PpIX solution prepared in acetone.

Compared to ALA and MALA, which require fresh preparation and pH adjustment, ALA/MALAAuNPs exhibit high stability. This enhanced stability streamlines the administration as contrast agents or in RDT therapy, making it more convenient and practical for patients and healthcare providers. GABAAuNPs can be produced at a lower cost than ALA/MALAAuNPs. This cost-effectiveness is essential for making diagnosis and therapy accessible.

Additional experiments will warranted to enhance the findings of this study. Employing higher-energy X-rays (>200 keV) could provide valuable insights into the effects of the ALA/MALA/GABAAuNPs. Additionally, substituting the MTS assay with clonogenic survival assays would offer a more comprehensive assessment of cell viability. Furthermore, quantifying reactive oxygen species (ROS) immediately following X-ray exposure could elucidate the role of ROS in mediating cell death. Moreover, incorporating a Cherenkov camera would enable real-time visualization and quantification of Cherenkov luminescence or luminescence of water, providing valuable information about the spatial distribution of radiation energy deposition. Ultimately, clinical trials are essential to establish the safety and efficacy of these ALA/MALA/GABAAuNPs in a clinical setting.

5. Conclusion

ALAAu, MALAAu and GABAAu nanoparticles were synthesized using photoreduction and exhibited excellent photophysical properties. Conjugation of ALA or MALA with nanoparticles allows their selective uptake by cancer cells due to the specific ALA transporters. Additionally, ALA/MALAAuNPs serve as radiosensitizers in RDT. GABAAuNPs can specifically bind to receptors overexpressed in breast cancer cells. When MCF-7 cells were incubated with ALAAuNPs and MALAAuNPs and then irradiated with 35 kV X-rays, cell viability was significantly reduced by approximately 22.9 % and 18.7 %, respectively, compared to non-irradiated cells. Incubation with GABAAuNPs resulted in a decrease in cell viability of about 9.7 % compared to non-irradiated cells. These results indicate the potential of these nanoparticles to enhance breast cancer screening tests and radiotherapy.

Conflict de interest

I declare that I have no conflicts of interest to disclose concerning this research or the publication of this paper.

CRediT authorship contribution statement

Isabela Santos Lopes: Investigation. **Noemy Rodrigues Santos:** Data curation, Investigation, Methodology. **Giovana Dias da Silva:** Data curation, Investigation, Methodology. **Leonardo Camargo dos Santos:** Methodology. **Maria da Penha Albuquerque Potiens:** Methodology, Supervision, Validation. **Daniel Perez Vieira:** Formal analysis, Methodology, Supervision, Validation. **Lilia Coronato Courrol:** Conceptualization, Formal analysis, Funding acquisition, Investigation, Methodology, Project administration, Resources, Supervision, Validation, Visualization, Writing – original draft, Writing – review & editing.

Declaration of competing interest

The authors declare that they have no known competing financial interests or personal relationships that could have appeared to influence the work reported in this paper.

Data availability

Data will be made available on request.

Acknowledgments

The authors would like to thank the Multi-user Centers of ABC Federal University (UFABC), Energy and Nuclear Research Institute (IPEN/CNEN-SP), The National Institute of Science and Technology Complex Fluids (INCT-FCX) grant 2014/50983-3 and São Paulo State Research Foundation, FAPESP grant 2022/14030-8.

References

Akram, M., Iqbal, M., Daniyal, M., Khan, A.U., 2017. Awareness and Current Knowledge of Breast Cancer Biological Research **50**.
Akter, Z., Khan, F.Z., Khan, M.A., 2023. Gold nanoparticles in triple-negative breast cancer therapeutics. Curr. Med. Chem. 30, 316–334.
Allen, N.C., Chauhan, R., Bates, P.J., O'Toole, M.G., 2022. Optimization of Tumor Targeting Gold Nanoparticles for Glioblastoma Applications Nanomaterials **12**.
Amina, S.J., Guo, B., 2020. A review on the synthesis and functionalization of gold nanoparticles as a drug delivery Vehicle. Int. J. Nanomed. 15, 9823–9857.
Arnold, M., Morgan, E., Rumgay, H., Mafra, A., Singh, D., Laversanne, M., Vignat, J., Gralow, J.R., Cardoso, F., Siesling, S., Soerjomataram, I., 2022. Current and future burden of breast cancer: global statistics for 2020 and 2040. Breast 66, 15–23.
Bilynsky, C., Millot, N., Papa, A.L., 2022. Radiation Nanosensitizers in Cancer Therapy-From Preclinical Discoveries to the Outcomes of Early Clinical Trials Bioengineering & Translational Medicine, vol. 7.
Blanco, K.C., Moriyama, L.T., Inada, N.M., Salvio, A.G., Menezes, P.F.C., Leite, E.J.S., Kurachi, C., Bagnato, V.S., 2015. Fluorescence Guided PDT for Optimization of the Outcome of Skin Cancer Treatment Frontiers in Physics, vol. 3.
Blum, N.T., Zhang, Y.F., Qu, J.L., Lin, J., Huang, P., 2020. Recent Advances in Self-Exciting Photodynamic Therapy Frontiers in Bioengineering and Biotechnology, vol. 8.
Brzozowska, A., Burdan, F., Duma, D., Solski, J., Mazurkiewicz, M., 2017. gamma-amino butyric acid (GABA) level as an overall survival risk factor in breast cancer. Ann. Agric. Environ. Med. 24, 435–439.
Casta, R., Champeaux, J.P., Moretto-Capelle, P., Sence, M., Cafarelli, P., 2015. Electron and photon emissions from gold nanoparticles irradiated by X-ray photons. J. Nanoparticle Res. 17.
Chen, Y., Yang, J., Fu, S.Z., Wu, J.B., 2020. Gold nanoparticles as radiosensitizers in cancer radiotherapy. Int. J. Nanomed. 15, 9407–9430.
Chen, X.Y., Yung, L.Y.L., Tan, P.H., Bay, B.H., 2022. Harnessing the Immunogenic potential of gold nanoparticle-based Platforms as a therapeutic Strategy in breast cancer Immunotherapy: a Mini review. Front. Immunol. 13.
Cline, B., Delahunty, I., Xie, J., 2019. Nanoparticles to mediate X-ray-induced photodynamic therapy and Cherenkov radiation photodynamic therapy. Wiley Interdisciplinary Reviews-Nanomedicine and Nanobiotechnology 11.
Diffey, J., 2017. How many physicists does it take to test a mammography unit? Australas. Phys. Eng. Sci. Med. 40, 1–6.
Fathy, M.M., Mohamed, F.S., Elbialy, N., Elshemey, W.M., 2018. Multifunctional Chitosan-Capped Gold Nanoparticles for enhanced cancer chemo-radiotherapy: an invitro study. Physica Medica-European Journal of Medical Physics 48, 76–83.
Fratoddi, I., Venditti, I., Cametti, C., Russo, M.V., 2015. How Toxic Are Gold Nanoparticles? the State-Of-The-Art Nano Research, vol. 8, pp. 1771–1799.
Glaser, A.K., Zhang, R.X., Andreozzi, J.M., Gladstone, D.J., Pogue, B.W., 2015. Cherenkov Radiation Fluence Estimates in Tissue for Molecular Imaging and Therapy Applications Physics in Medicine and Biology, vol. 60, pp. 6701–6718.
Goncalves, K.D., da Silva, M.N., Sicchieri, L.B., Silva, F.R.D., de Matos, R.A., Courrol, L. C., 2015. Aminolevulinic Acid with Gold Nanoparticles: a Novel Theranostic Agent for Atherosclerosis Analyst **140** 1974-80.
Goncalves, K.D., Vieira, D.P., Levy, D., Bydlowski, S.P., Courrol, L.C., 2020. Uptake of Silver, Gold, and Hybrids Silver-Iron, Gold-Iron and Silver-Gold Aminolevulinic Acid Nanoparticles by MCF-7 Breast Cancer Cells Photodiagnosis and Photodynamic Therapy **32**.
Goncalvez, K.D., Vieira, D.P., Courrol, L.C., 2018. Study OF THP-1 MACROPHAGE viability after SONODYNAMIC therapy using methyl ESTER OF 5-AMINOLEVULINIC acid gold nanoparticles. Ultrasound Med. Biol. 44, 2009–2017.
Gonzales, J., Wang, F., Zamora, G., Trinadad, A., Marcu, L., Cherry, S., Hirschberg, H., 2014. Conference on Optical Techniques in Neurosurgery, Neurophotonics, and Optogenetics, Series 8928. San Francisco, CA, Feb 01-04 2014) (Proceedings of SPIE.
Gutowski, M., Kowalczyk, S., 2013. A study of free radical chemistry: their role and pathophysiological significance. Acta Biochim. Pol. 60, 1–16.
Hon, J.D.C., Singh, B., Sahin, A., Du, G., Wang, J.H., Wang, V.Y., Deng, F.M., Zhang, D. Y., Monaco, M.E., Lee, P., 2016. Breast cancer molecular subtypes: from TNBC to QNBC. Am. J. Cancer Res. 6, 1864–1872.
Hsu, J.C., Nieves, L.M., Betzer, O., Sadan, T., Noel, P.B., Popovtzer, R., Cormode, D.P., 2020. Nanoparticle Contrast Agents for X-Ray Imaging Applications Wiley Interdisciplinary Reviews-Nanomedicine and Nanobiotechnology, vol. 12.
Ismael, F.S., Amasha, H., Bachir, W., 2020. Optimized Cylindrical Diffuser Powers for Interstitial PDT Breast Cancer Treatment Planning: A Simulation Study Biomed Research International **2020**.
Janssen, S., Kasmann, L., Fahlbusch, F.B., Rades, D., Vordermark, D., 2018. Side Effects of Radiotherapy in Breast Cancer Patients the Internet as an Information Source Strahlentherapie Und Onkologie **194** 136-42.
Kuncic, Z., Lacombe, S., 2018. Nanoparticle Radio-Enhancement: Principles, Progress and Application to Cancer Treatment Physics in Medicine and Biology, vol. 63.

Kurapov, P.B., Bakhtenko, E.Y., 2018. Gold nanoparticles. In: THE DIAGNOSIS and TREATMENT of CANCER Bulletin of Russian State. Medical University, pp. 86–93.
Lebron-Zapata, L., Jochelson, M.S., 2018. Overview of Breast Cancer Screening and Diagnosis Pet Clinics **13** 301-+.
Lorente-Ramos, R.M., Arman, J.A., 2022. Review of Contrast-Enhanced Mammography Contemporary Diagnostic Radiology, vol. 45.
Mateus, J.E., Valdivieso, W., Hernandez, I.P., Martinez, F., Paez, E., Escobar, P., 2014. Cell Accumulation and Antileishmanial Effect of Exogenous and Endogenous Protoporphyrin IX after Photodynamic Treatment Biomedica, vol. 34, pp. 589–597.
Nagi, N.M.S., Khair, Y.A.M., Abdalla, A.M.E., 2017. Capacity of Gold Nanoparticles in Cancer Radiotherapy Japanese Journal of Radiology, vol. 35, pp. 555–561.
Noor, F., Noor, A., Ishaq, A.R., Farzeen, I., Saleem, M.H., Ghaffar, K., Aslam, M.F., Aslam, S., Chen, J.T., 2021. Recent Advances in Diagnostic and Therapeutic Approaches for Breast Can- Cer: A Comprehensive Review Current Pharmaceutical Design, vol. 27, pp. 2344–2365.
Perry, H., Phillips, J., Dialani, V., Slanetz, P.J., Fein-Zachary, V.J., Karimova, E.J., Mehta, T.S., 2019. Contrast-enhanced mammography: a Systematic Guide to Interpretation and reporting. Am. J. Roentgenol. 212, 222–231.
Piccolo O, Ha M, Robar J, Lincoln J, Melong N, Berman J, Fernandez N, Orr B and Borsavage J 2022 RADIATION DOSE ENHANCEMENT USING GOLD NANOPARTICLES with A DIAMOND LINEAR ACCELERATOR TARGET: A MULTIPLE CELL TYPE ANALYSIS Radiotherapy and Oncology **174** S38-S.
Sachar, M., Anderson, K.E., Ma, X.C., 2016. Protoporphyrin IX: the good, the Bad, and the Ugly. J. Pharmacol. Exp. Therapeut. 356, 267–275.
Schulz-Wendtland, R., Wenkel, E., Wacker, T., Hermann, K.P., 2009. Quo vadis? Trends in Digital mammography Geburtshilfe Und Frauenheilkunde, 69, 108–117.
Shaffer, T.M., Pratt, E.C., Grimm, J., 2017. Utilizing the power of Cerenkov light with nanotechnology. Nat. Nanotechnol. 12, 106–117.
Swaminathan, H., Saravanamurali, K., Yadav, S.A., 2023. Extensive Review on Breast Cancer its Etiology, Progression, Prognostic Markers, and Treatment Medical Oncology, vol. 40.
Takahashi, J., Misawa, M., Murakami, M., Mori, T., Nomura, K., Iwahashi, H., 2013. 5-Aminolevulinic Acid Enhances Cancer Radiotherapy in a Mouse Tumor Model Springerplus, vol. 2.
Torrisi, L, Restuccia, N, Torrisi, A, 2019. Study of gold nanoparticles for mammography diagnostic and radiotherapy improvements *Reports of Practical*. Oncol. Radiother. 24, 450–457.
Wu, L., Zhang, Y., Zheng, C.L., Zhao, F.Q., Lin, Y., 2023. Gamma-aminobutyric acid type A receptor Subunit Delta (GABRD) Inhibits breast cancer Progression by Regulating the cell Cycle. Iran. J. Public Health 52, 542–552.
Xu, L.N., Xu, M., Sun, X., Feliu, N., Feng, L.X., Parak, W.J., Liu, S.J., 2023. Quantitative comparison of gold nanoparticle delivery via the enhanced permeation and retention (EPR) effect and Mesenchymal Stem cell (MSC)-Based targeting. ACS Nano 17, 2039–2052.
Yamamoto, S., 2021. Discovery of the luminescence of water during irradiation of radiation at a lower energy than the Cherenkov light threshold. Radiol. Phys. Technol. 14, 16–24.
Yamamoto, S., Koyama, S., Komori, M., Toshito, T., 2016. Luminescence imaging of water during irradiation of X-ray photons lower energy than Cerenkov- light threshold. Nucl. Instrum. Methods Phys. Res. Sect. A Accel. Spectrom. Detect. Assoc. Equip. 832, 264–270.
Yamamoto, S., Koyama, S., Yabe, T., Komori, M., Tada, J., Ito, S., Toshito, T., Hirata, Y., Watanabe, K., 2018. Stability and linearity of luminescence imaging of water during irradiation of proton-beams and X-ray photons lower energy than the Cerenkov light threshold. Nucl. Instrum. Methods Phys. Res. Sect. A Accel. Spectrom. Detect. Assoc. Equip. 883, 48–56.
Yang, X., Palasuberniam, P., Kraus, D., Chen, B., 2015. Aminolevulinic acid-based tumor detection and therapy: molecular mechanisms and Strategies for enhancement. Int. J. Mol. Sci. 16, 25865–25880.
Yang, D.M., Cvetkovic, D., Chen, L.L., Ma, C.M.C., 2022. Therapeutic effects of in-vivo radiodynamic therapy (RDT) for lung cancer treatment: a combination of 15MV photons and 5-aminolevulinic acid (5-ALA). Biomedical Physics & Engineering Express 8.
Yang, L.P., Zhu, J., Wang, L.L., He, L.B., Gong, Y., Luo, Q.F., 2023. A novel risk score model based on gamma-aminobutyric acid signature predicts the survival prognosis of patients with breast cancer. Front. Oncol. 13.
Zhang, Z.X., Wang, S.J., Xu, H., Wang, B., Yao, C.P., 2015. Role of 5-aminolevulinic acid-conjugated gold nanoparticles for photodynamic therapy of cancer. J. Biomed. Opt. 20, 8.